

Example-based Image Colorization via Automatic Feature Selection and Fusion

Bo Li

School of Mathematics and Information Sciences, Nanchang Hangkong University, Nanchang, China.

Yu-Kun Lai, Paul L. Rosin

School of Computer Science and Informatics, Cardiff University, UK

Abstract

Image colorization is an important and difficult problem in image processing with various applications including image stylization and heritage restoration. Most existing image colorization methods utilize feature matching between the reference color image and the target grayscale image. The effectiveness of features is often significantly affected by the characteristics of the local image region. Traditional methods usually combine multiple features to improve the matching performance. However, the same set of features is still applied to the whole images. In this paper, based on the observation that local regions have different characteristics and hence different features may work more effectively, we propose a novel image colorization method using automatic feature selection with the results fused via a Markov Random Field (MRF) model for improved consistency. More specifically, the proposed algorithm automatically classifies image regions as either uniform or non-uniform, and selects a suitable feature vector for each local patch of the target image to determine the colorization results. For this purpose, a descriptor based on luminance deviation is used to estimate the probability of each patch being uniform or non-uniform, and the same descriptor is also used for calculating the label cost of the MRF model to determine which feature vector should be selected for each patch. In addition, the similarity between the luminance of the neighborhood is used as the smoothness cost for the MRF model which

Email addresses: libo@nchu.edu.cn (Bo Li), Yukun.Lai@cs.cardiff.ac.uk, Paul.Rosin@cs.cf.ac.uk (Yu-Kun Lai, Paul L. Rosin)

enhances the local consistency of the colorization results. Experimental results on a variety of images show that our method outperforms several state-of-the-art algorithms, both visually and quantitatively using standard measures and a user study.

Keywords: image colorization, automatic feature selection, Markov random field, Bayesian inference

1. Introduction

The aim of example-based image colorization is to transfer the chrominance information from a reference image with color to a target grayscale image. It is an important research topic in image processing, and has many applications in different areas, such as heritage restoration [1] and image stylization [2, 3]. However, it is ill-posed and difficult because the common grayscale information between the reference and target images may not be sufficiently distinctive for reliable transfer. Most existing image colorization methods use feature matching: given a reference image with color information, the target grayscale image will be colorized by finding correspondences from the reference image based on feature similarity. Therefore, choosing suitable features is key to the colorization performance. In the pioneering work by Welsh et al. [4], luminance features are used to find the correspondences. However, such features perform poorly for non-uniform (e.g. textured) regions, leading to artifacts in the colorized images. More recent work has used many advanced texture features for image colorization, such as Gabor wavelets [5], SIFT [6], SURF [7], etc. To improve results, most existing methods use multiple features as a combined vector for matching, which implies that individual features contribute *equally* to region matching across the entire image. However, a specific type of feature is often more effective for certain types of regions. It is thus beneficial to treat regions *differently* according to their local characteristics. For example, pixels in uniform regions are more suitable to be matched by intensity features whereas texture descriptors should be used for highly non-uniform regions. An example is shown in Fig. 1. We can see that the intensity feature is suitable for the sky region but not the castle (Fig. 1(f)), whereas the texture descriptor performs well for the non-uniform castle regions but produces erroneous matches in the uniform

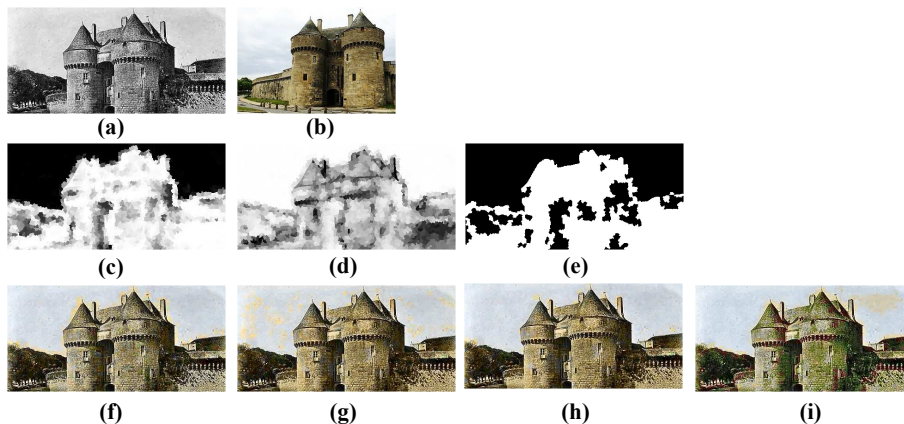


Figure 1: Illustration of automatic feature selection for colorization. (a) target grayscale image, (b) reference color image, (c)(d) probability maps of uniform and non-uniform regions (black to white for 0 to 1), (e) the optimal label image learned by an MRF model (black: uniform, white: non-uniform), (f)(g): colorization results using intensity feature and SURF texture feature respectively, (h) colorization result using our proposed automatic feature selection and fusion, (i) the result using direct combination of intensity and SURF texture features.

25 regions (Fig. 1(g)). Combining these two features improves the result (Fig. 1(i)), but numerous matching errors remain which lead to the green tint on the castle and the yellow tint in the sky. Our automatic feature selection and fusion is effective at avoiding such problems (Fig. 1(h)).

In this paper, we propose a novel image colorization method via automatic fea-
 30 ture selection within a Markov Random Field (MRF) framework. To the best of our knowledge, this is the first work that exploits automatic feature selection and fusion for image colorization. Specifically, image regions can be generally classified as being uniform or non-uniform. In uniform regions, the luminance of pixels is evenly distributed, so the intensity distribution can represent these regions well, whereas in non-uniform regions, texture feature descriptors are effective to represent the patterns. Based on
 35 the learned distribution of intensity deviation for uniform and non-uniform regions, the probability of a given region being assigned a uniform or non-uniform label is estimated using Bayesian inference, which is then used for selecting suitable features. Instead of making individual decisions locally, we further develop an MRF model to

40 improve the labeling consistency where the probability is used for the label cost and
similarity between the luminance of the neighboring regions for the smoothness cost.
The MRF model can be efficiently solved by the graph cut algorithm, enhancing the lo-
cal consistency of the colorization result. Finally, the colorization results are obtained
by transferring corresponding chrominance information from the reference image to
45 the target grayscale image.

The main contributions of the paper are summarized as follows: 1) We propose a
novel approach to improving image colorization by local feature selection and fusion.
2) We develop a novel algorithm that classifies local image regions into uniform and
non-uniform regions and applies suitable features. An MRF framework guided by
50 Bayesian probability inference is further proposed to improve locality coherence. 3)
We perform extensive experimental analysis both visually and quantitatively, which
shows that the proposed method outperforms state-of-the-art methods.

The rest of this paper is organized as follows. We review work most relevant to this
paper in Sec. 2, and then describe the proposed algorithm in detail in Sec. 3. Experi-
55 mental results are shown in Sec. 4 and finally conclusions are drawn in Sec. 5.

2. Related Work

In general, existing image colorization methods can be divided into three cate-
gories: user-scribble based methods, example-based methods and methods that use a
large number of training images. User-scribble based methods are semi-automatic, and
60 they often require substantial user interaction as input. In the pioneering work by Levin
et al. [8], some color scribbles on the target image are required as input, and then the
color will be propagated based on least squares diffusion. However, there are obvious
color bleeding effects around edges due to the isotropic nature of the diffusion. In order
to better preserve the edge structure, an adaptive edge detection based colorization al-
65 gorithm was proposed in [9]. To make the color region boundaries more consistent with
human judgement, a saliency guided colorization technique was proposed in [10]. The
approach first generates a saliency map of the reference and target images to predict the
visual attention of human viewers, softly segmenting the images into foreground and

background regions. Color transfer is then performed first to the foreground and then
70 the background using a weighted color transfer algorithm. In [11], a fast colorization
method based on the geodesic distance weighted chrominance blending was proposed.
Thanks to the use of luminance-weighted chrominance blending model and efficient
intrinsic distance computation, the method is efficient for both image and video col-
orization. However, for all these scribble-based methods, it is time-consuming and the
75 quality of colorization results highly depends on the appropriateness of user scribbles.

Compared with user-scribble based methods, example-based methods can be fully
automatic without any user interaction. For example-based methods, typically only
one reference image with color information is needed, and the target grayscale image
is colorized automatically. The pioneering work by Welsh et al. [4] first finds the
80 best matching sample in the reference image for each pixel in the target image, and
then the chrominance information is transferred to the target grayscale image from the
color reference image by the matching results to form the colorized images. Most of
the existing example-based colorization algorithms follow this framework involving
the steps of feature matching and color transfer. As feature matching is critical to
85 the quality of results and the proposed method, Welsh’s method resorts to manually
specified swatches when automatic matching fails to produce satisfactory results.

In order to improve the feature matching performance, different features or different
combinations of features have been proposed. Ying et al. [12] proposed using a more
extensive neighborhood descriptor computed using co-occurrence matrix based texture
90 features. To reduce artifacts caused by outliers, the edit-nearest-neighbor method [13]
is used to try to remove the outliers. While the paper presents examples showing im-
proved results, the co-occurrence matrix is expensive to compute. Chen et al. [14]
combined [4] with foreground/background image matting to improve the colorization
results but user interaction is needed to guide the grayscale image matting. Most of the
95 existing methods focus on finding a proper combination of features for the *whole* im-
age, rather than *selecting* proper features for each local pixel or region, as we propose
to do in this paper.

As the methods above match each pixel in isolation, spatial consistency cannot
be guaranteed in general. In order to enhance locality consistency and reduce color

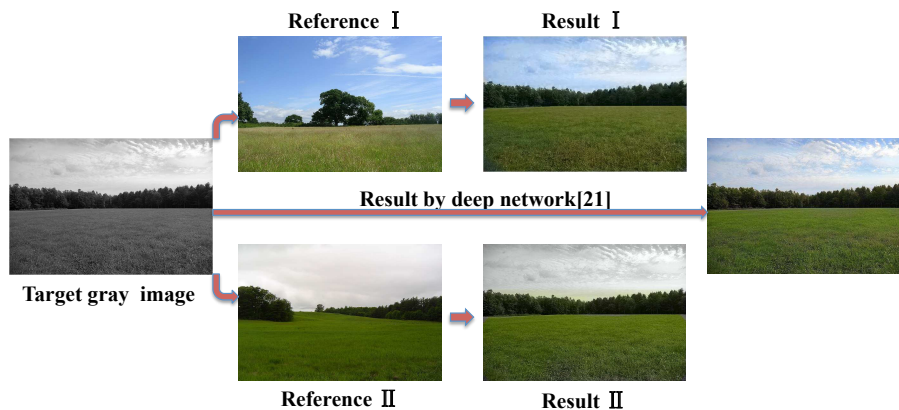


Figure 2: Colorization results with different reference images. While all the colorized images look plausible, our method is able to produce different colorized images based on different reference images. In comparison, deep learning based method [18] can only produce one output.

100 bleeding effects at edges, an edge-preserving total variation based image colorization algorithm was proposed in [15]. However, since only chrominance information is involved in the variational formulation, the results of [15] suffer from halo effects near strong contours. In [16], a coupled regularization term with luminance and chrominance channels is introduced to preserve image contours during the colorization process. The method produces colorization results which are better aligned with edge structures. However, significant artifacts can still be produced by incorrect feature matching. Compared with the local matching based methods, a novel global colorization method based on histogram regression was proposed in [17]. The basic assumption is that the final colorized image should have a similar color distribution as the reference image, and color matching is conducted by finding and adjusting the zero-points of the color histogram. The method however may not work well for complicated scenarios where the color mapping cannot be effectively represented using global histograms.

An alternative category of approaches resorts to a large number of training images. For example, the proliferation of internet images can be utilized for image colorization. In [19, 20, 21], target grayscale images are colorized by internet images. The reference images are searched from the internet based upon a semantic label given by

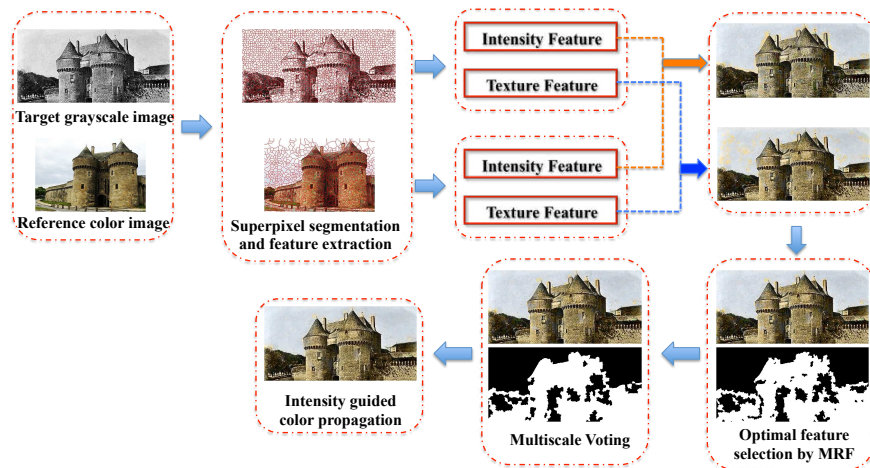


Figure 3: The pipeline of the proposed method.

the user and from the vast number of returned images a subset is chosen by means of a combined similarity metric. However, it is computationally expensive and depends on the accuracy of the semantic segmentation. Recently, deep learning based methods
120 have been proposed for image colorization [6, 7, 18, 22] and produce promising results. However, unlike example-based methods, the colorization results cannot be controlled by users. Since image colorization is essentially an ill-posed problem: the target images can often be naturally colorized in different ways due to semantic ambiguities and style preference. One example is shown in Fig. 2. We can see that given different style
125 reference images, our method, as an example-based method, can generate multiple distinct and plausible colorization results (e.g. the sky can be blue for a sunny day or gray for a cloudy day), while the recent deep learning based method [18] does not provide flexible control and can only produce one output image.

In this paper, a novel example-based image colorization method is proposed. Unlike existing methods, we aim to automatically find suitable features for each local
130 region rather than using the same feature for the whole image globally. We further propose an MRF framework to solve feature selection and locality consistency simultaneously, which can be efficiently solved using the graph cut algorithm. As we will show later, our automatic feature selection helps to significantly improve feature matching,

135 and thus provides an effective solution to a major challenge of image colorization.

3. Our Method

The pipeline of the proposed algorithm is shown in Fig. 3. In order to suppress the influence of global luminance difference between the reference and target images, a global linear luminance remapping to the reference image is applied as in [4]. For computational efficiency, and to help improve the spatial consistency of the results, 140 both the reference and target images are segmented into superpixels, and intensity and texture features are extracted from each superpixel. Using either of these features, we can find the corresponding best matching result for each target superpixel based on the Euclidean distance in the feature space (efficiently computed using the ANN 145 library [23]). Then a two-label MRF model is formulated to choose the optimal correspondence according to different features, based on the probability of superpixels belonging to uniform or non-uniform regions. Following the initial labeling, a multi-scale voting process is performed to eliminate the isolated outliers and enhance locality consistency. Finally, the chrominance channels are filtered by the standard guided fil- 150 ter [24] with the guidance of the luminance channel.

3.1. Image Segmentation and Feature Extraction

For example-based image colorization, the most time-consuming step is finding the correspondence from the reference color image for each pixel in the target grayscale image. It is computationally expensive, especially when the feature dimensionality is 155 high. On the other hand, neighboring pixels in natural images often share similar characteristics, and can be processed simultaneously and in the same manner. As we will demonstrate later, doing so also ensures coherent colorization in local neighborhoods and reduces mismatches. Based on the above observation, both the reference image and the target grayscale image are first segmented into superpixels. For the reference 160 image, superpixel segmentation is performed using the color information, whereas the target grayscale image is segmented using the luminance information only. In this paper, we adopt the Turbopixel algorithm [25], which can process color and grayscale

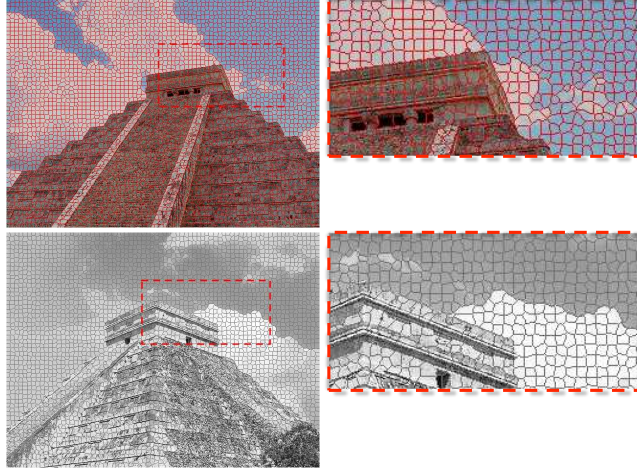


Figure 4: Examples of superpixel segmentation shown with magnified selection.

images while preserving the edge structure well. The superpixel number is set to 4000
in our experiments which provides a good balance between efficiency and quality, as
165 we will demonstrate later. Note that the required number of superpixels depends on
the image content, rather than its resolution. Fig. 4 shows the superpixel segmentation
results for both color and grayscale images. From the magnification of the boundary
areas, we can see that the edge structure is well preserved.

For each superpixel from the reference color image and the target grayscale image,
170 two types of features are extracted:

Intensity feature. The intensity feature we used is a 27-dimensional vector computed
based on the luminance value. It is composed of three parts: the mean intensity within
the superpixel (\bar{l}_1), the mean intensity of the neighboring superpixels (\bar{l}_2) and the in-
tensity distribution within the superpixel (\mathbf{h}_l), where $\bar{l}_2 = \frac{1}{|\mathcal{N}_i|} \sum_{j \in \mathcal{N}_i} \bar{l}_1(j)$ and \mathcal{N}_i
175 is the set of neighboring superpixels of the i^{th} superpixel. The intensity distribution \mathbf{h}_l
is a histogram of the intensity distribution within each superpixel. In our experiments,
the intensity range 0–255 is divided into 25 bins, and each entry represents the propor-
tion of the pixels whose the intensity is in the range of the bin compared with the total
number of pixels in the superpixel. The intensity feature is denoted as \mathbf{f}^I .

180 **Texture feature.** In this paper, the scale-invariant and rotation-invariant SURF feature [26] is used as the texture descriptor. At each pixel a 128-dimensional SURF descriptor is extracted, and then the average SURF feature within the superpixel is computed as the texture feature of the superpixel. We denote the texture feature as \mathbf{f}^T .

185 These intensity and texture features are chosen because they are representative for their feature types and produce competitive results (see also the comparative results between our method and state-of-the-art methods). Since the focus of this paper is novel feature selection and fusion, these elementary features are fixed, although our method can be directly combined with alternative features. To help choose intensity or texture feature for matching, the intensity standard deviation d_i within each superpixel i is also computed. A small value of the standard deviation implies that the intensity distribution within the superpixel is even. The standard deviation is used for automatic selection of features (see the next subsection for detail), rather than finding the best candidate.

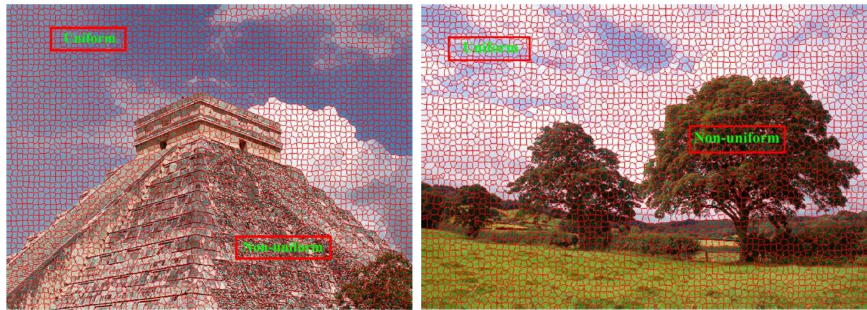


Figure 5: Examples of training samples from uniform and non-uniform regions.

3.2. MRF-based Automatic Feature Selection

195 In this subsection, we discuss our novel automatic feature selection for image colorization. The intuition is that different regions can be better represented by different features. In general, a natural image can be decomposed into uniform and non-uniform regions. We use the term non-uniform in a broad sense to refer to regions containing sufficient details, to allow texture descriptors to work effectively. This is different from

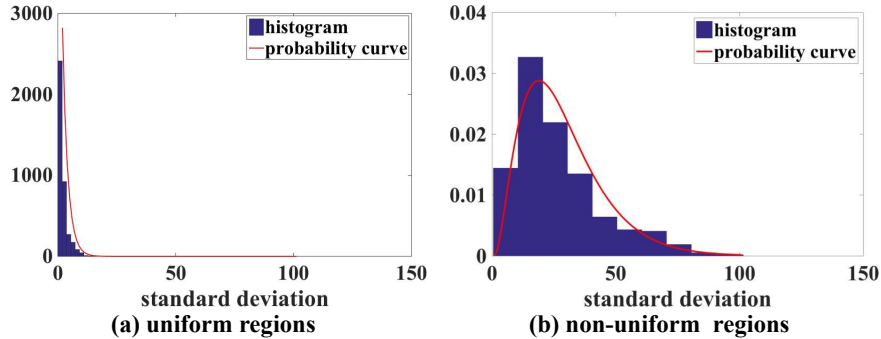


Figure 6: The histograms of standard deviation of superpixels extracted from uniform and non-uniform training examples, and their fitted Gamma distributions.

200 the standard texture/non-texture classification [27, 28] so we develop a simple approach for our purpose. In uniform regions, the luminance of pixels is evenly distributed, and the intensity feature \mathbf{f}^I can represent these regions well. While in non-uniform regions, texture feature descriptors \mathbf{f}^T are a good choice to represent repeated patterns. One of the main contributions of this paper is to design an automatic feature selection framework for each superpixel within an MRF framework. In addition to feature selection, 205 locality consistency can also be simultaneously enhanced by the MRF model.

3.2.1. Probability Estimation for Region Uniformity

When the superpixel segmentation is dense enough, the intensity standard deviation of each superpixel can be seen as a good descriptor to determine its characteristics, i.e. 210 smaller deviation implies uniform while bigger value means non-uniform. Therefore we adopt intensity standard deviation as the feature variable to estimate the probability distribution of each type of region.

In this paper, Bayesian inference is used to determine the probability of each superpixel belonging to each type of region. For the i^{th} superpixel x_i , given its corresponding standard deviation d_i , we denote its probability of belonging to a uniform region as $P(x_i \in U|d_i)$. Using Bayesian inference, the posterior probability can be computed by

$$P(x_i \in U|d_i) = \frac{P(U)P(d_i|x_i \in U)}{P(U)P(d_i|x_i \in U) + P(N)P(d_i|x_i \in N)}, \quad (1)$$

where $P(U)$ (or $P(N)$) denotes the a priori probability for a region to be uniform (or non-uniform), and $P(d_i|x_i \in U)$ (or $P(d_i|x_i \in N)$) is the conditional probability of having given standard deviation d_i for a region known as uniform (or non-uniform). In general, we assume uniform and non-uniform regions are equally common and the a priori probabilities $P(U)$, $P(N)$ can be set as 0.5.

In order to estimate the conditional probability $P(d_i|x_i \in U)$ and $P(d_i|x_i \in N)$, we create a training set by manually selecting superpixels from uniform and non-uniform regions, and calculating the corresponding standard deviation values. In this paper, we collected 3000 superpixels for each type of region from 10 images, which are sufficient to estimate the distributions of standard deviation. An example is shown in Fig. 5. The histograms of the standard deviation for uniform and non-uniform regions are shown in Fig. 6. The shape of the histogram can be well approximated by a Gamma distribution

$$\Gamma(\alpha, \beta) = \frac{\beta^\alpha x^{\alpha-1} e^{-x\beta}}{\Gamma(\alpha)} \quad (2)$$

where α and β are the shape and scale parameters of the Gamma distribution. Given our training samples, the Gamma distributions fitted are shown in Fig. 6, with the parameters for uniform regions and non-uniform regions being: $\{\alpha_U = 0.9544, \beta_U = 2.3424\}$ and $\{\alpha_N = 2.8295, \beta_N = 9.8095\}$.

Given a superpixel with luminance standard deviation d_i , its probability of belonging to uniform regions $P(x_i \in U|d_i)$ can be computed using Eqn. 1. We can similarly compute its probability of belonging to non-uniform regions $P(x_i \in N|d_i)$, which satisfies $P(x_i \in U|d_i) + P(x_i \in N|d_i) = 1$. The probability of uniformity is also useful for feature matching as uniform regions should generally be colorized using samples from uniform regions, and the same for non-uniform regions. We thus add $P(x_i \in U|d_i)$ to each type of the features introduced in the previous section which serves as a soft constraint.

3.2.2. MRF-based Labeling for Feature Selection

With the estimated posterior probability, a trivial way of labeling superpixels as uniform or non-uniform is thresholding. Such approach however does not take into account spatial consistency. In this paper, we propose a novel automatic feature selection

approach for image colorization within an MRF framework. For each superpixel in the
 target image, we can find two matched superpixels from the reference image based on
 the intensity and texture features. The searching process can be efficiently performed
 using the approximate nearest neighbour (ANN) tree searching algorithm [23]. An ex-
 ample is shown in Fig. 1. We can see that the intensity features perform well within
 uniform regions (Fig. 1(f)), whereas the texture descriptor is effective at non-uniform
 regions (Fig. 1(g)). Most existing methods combine these two types of features as
 a combined feature and use the same searching process in both cases. The result as
 shown in (Fig. 1(i)) still contains many incorrect matching results. Rather than com-
 bining the two features, in this paper we assume that for each superpixel the matching
 result is determined by only the single optimal feature. We assume that in uniform
 regions the colorization should be determined by the intensity feature, whereas in
 non-uniform regions the texture feature should be dominant. Therefore, the problem of
 feature selection can be regarded as a binary labeling problem, where label 0 denotes
 intensity feature and label 1 means texture feature.

Let us denote the i -th superpixel in the target image as x_i , and the set of all su-
 perpixels in the target image as Ω . \mathcal{N} represents the set of adjacent superpixel pairs.
 The task of feature selection is to divide the whole set Ω into two disjoint sets, Ω_I
 for regions determined by intensity features and Ω_T for regions determined by texture
 features. The binary labeling problem can be formulated as the minimization of the
 following MRF energy function

$$\min_{\mathbf{S}} E(\mathbf{S}) = \sum_{i \in \Omega} D(S_i) + \lambda \sum_{(i,j) \in \mathcal{N}} f(S_i, S_j), \quad (3)$$

where S_i is the label for the i -th superpixel, which takes 0 or 1 to indicate whether the
 intensity feature or the texture feature is selected.

The first term $D(S_i)$ is the label cost which measures the cost to assign label S_i
 to the i -th superpixel x_i . Based on our assumption, the label cost of each superpixel
 should be determined by its probability of belonging to either the uniform regions or

non-uniform regions, i.e. the posterior probabilities:

$$D(S_i) = \begin{cases} P(x_i \in N|d_i) & \text{if } S_i = 0, \\ P(x_i \in U|d_i) & \text{if } S_i = 1. \end{cases} \quad (4)$$

The second term $f(S_i, S_j)$ is the pairwise term, which indicates the cost for assigning label S_i to the i -th superpixels while assigning label S_j to the j -th superpixel. In this paper, the pairwise term is defined as

$$f(S_i, S_j) = \begin{cases} 0, & \text{if } S_i = S_j \\ s(i, j), & \text{otherwise} \end{cases} \quad (5)$$

where $s(i, j)$ describes the similarity between adjacent superpixels. For improved coherence, we assume that neighboring superpixels with similar intensity values are likely to have the same label. Therefore, the function $s(i, j)$ is defined as follows:

$$s(i, j) = \exp \left\{ -\frac{\|\mathbf{c}_i - \mathbf{c}_j\|^2}{2\sigma_1^2} \right\} \exp \left\{ -\frac{(\bar{l}_1(i) - \bar{l}_1(j))^2}{2\sigma_2^2} \right\}, \quad (6)$$

where \mathbf{c}_i and $\bar{l}_1(i)$ are the central location and the mean intensity of the i -th superpixel. σ_1, σ_2 are parameters set as $\sigma_1 = 100$ and $\sigma_2 = 1$ (for images with approximately 1 megapixels). From the definition, the pairwise costs only exist for adjacent superpixels with different labels, and the effect is determined by the similarity between superpixels: i.e., the cost will be big if different labels are assigned to nearby superpixels with high similarity. Therefore, the main effect of the pairwise term is to enhance locality consistency, which is important for colorization.

Given the label cost and the pairwise terms, the two-label MRF model (3) can be optimized by the graph cut algorithm [29, 30]. Since our energy function is not sub-modular, the alpha-beta swap algorithm is adopted, which randomly selects two labels from the label set and tries to reduce the energy by swapping these labels. The algorithm is efficient, and runtime is less than 0.1 s for 4000 superpixels.

Finally, feature selection is determined by the labeling. For regions with label 0, i.e., uniform regions, the intensity feature is used for feature matching. Otherwise, the texture feature is used. Fig. 1 shows the colorization result by the proposed feature selection method. (c) and (d) are the corresponding label costs for the intensity

feature and the texture feature. (f) and (g) are the corresponding best matches using intensity and texture features, respectively. (e) is the optimal labeling obtained by the MRF model and (h) is the final colorization result. Our feature selection performs significantly better than using individual features, or their simple combination as shown in (i).

3.3. Consistency enhancement by multiscale voting

Although locality consistency has been taken into account in the MRF energy function, there still exist isolated wrong matches as shown in Figure 7(a). In order to improve the color consistency, a multiscale voting is further performed. The basic intuition is that the label assignment for a superpixel is likely to be wrong if most of its neighboring superpixels with similar image properties are assigned another label. Therefore, we can exploit neighboring superpixels to identify and correct invalid label assignments.

The target image is also oversegmented to produce coarse-scale superpixels by the Turbopixels method. In this paper, the number of coarse-scale superpixels is chosen as a quarter of the original superpixel segmentation. For each superpixel in the coarse scale, the final label is determined by the majority label obtained in the fine scale. Finally, median filtering is applied for the chrominance channels in the lab color space such that the color of each superpixel is replaced by the median of its neighboring superpixels, to further enhance color consistency. The result of multiscale voting is shown in Fig. 7(b). From the magnified selection, we can see that many isolated wrong matches are corrected.

3.4. Color propagation by guided filter

Although the multiscale voting process can reduce isolated matching errors, the resulting color images still show block effects as chrominance information is transferred on a superpixel basis, and can have quite a few sparse outliers, as shown in Fig. 8(a). Different from other image processing tasks, the target grayscale image is accurate for image colorization. Therefore, the intensity information of the target image can be

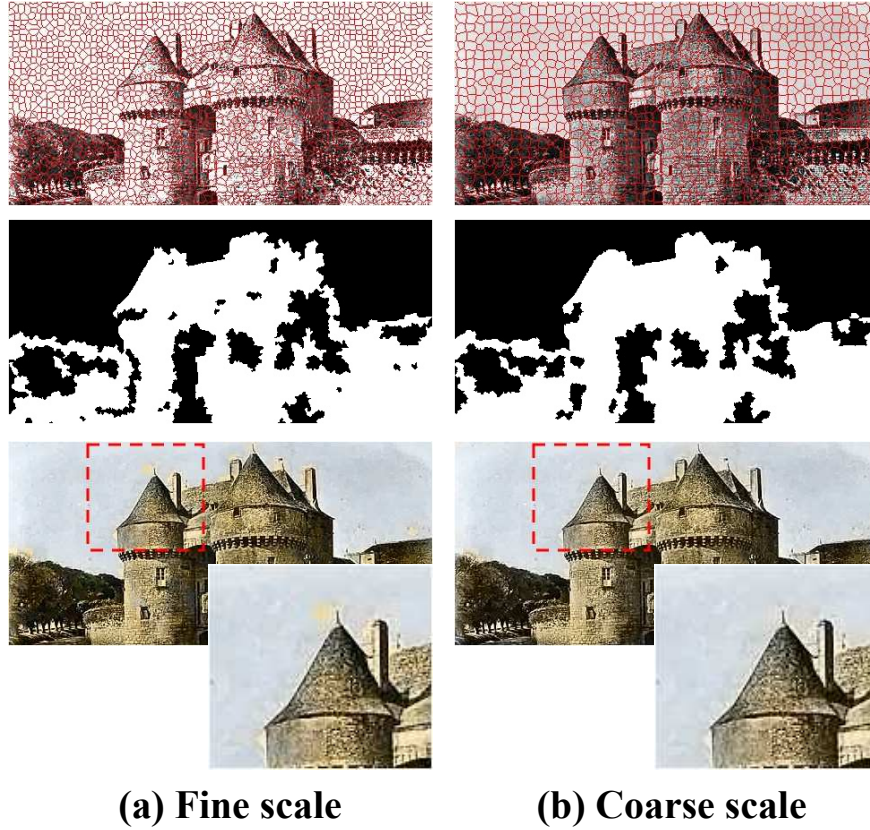


Figure 7: Example of multiscale voting. (a) fine scale matching without multiscale voting, (b) result with multiscale voting. From top to bottom: fine and coarse scale superpixels, uniform/non-uniform labels without and with multiscale voting, and colorization results without and with multiscale voting.

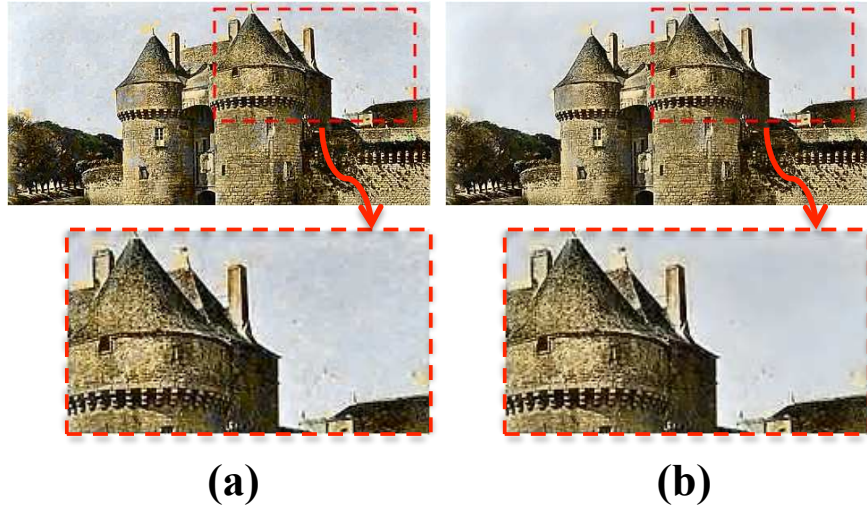


Figure 8: Example of luminance guided image filtering. (a) the original matching result, (b) the result after guided image filtering.

295 used to enhance the results, by exploiting the fact that nearby pixels with similar intensity values should come with similar colors. For this purpose, we adopt the guided filter [24] for color propagation where the target grayscale image is used as guidance, which is an edge-preserving smoothing operator which better utilizes the structures in the guidance image.

$$\mathbf{J}^* = \sum_j \mathbf{W}_{ij}(\mathbf{I})\mathbf{J}_j \quad (7)$$

300 where \mathbf{I} means the target grayscale image which is used as the guidance image, \mathbf{J} is the obtained chrominance channel from the last step, and \mathbf{W} is the adapted weight function as defined in [24]. The filtered image is shown in Fig. 8(b). We can see that block effects are smoothed while the edge information is preserved well.

4. Experiments

305 In this section, experimental results are presented to evaluate the performance of the proposed method, and compare it with several state-of-the-art methods [15, 16, 17]. In

order to make a fair comparison, the results of [17] are generated using the code provided by the author, and the results of [15] and [16] are provided by the authors. The results of different algorithms are evaluated both by visual inspection and by quantitative evaluation. In addition to example-based methods, two of the latest deep learning based methods [18, 22] are also included for visual comparison, using the code provided by authors. Since the standard quantitative measures we used to compare the results are not designed for the task of image colorization, in order to get fair and reliable comparison, a user study is also performed. The experiments were carried out on a computer with an Intel i7 2.8GHz CPU and 16GB memory.

4.1. Visual inspection

Thirteen natural images of different types, e.g., landscape, animals, and buildings, are chosen for the experiment. The colorization results are shown in Fig. 9. In order to evaluate the performance of automatic feature selection, the colorization results using the combined intensity and texture features are also presented as a baseline. From visual inspection, we can see that in most cases the proposed algorithm achieves the best results compared against the other four methods. In particular, our method substantially reduces wrong color matches, especially between uniform and non-uniform regions.

Method [17] is based on finding and adjusting the zero-points of the histograms of both the reference and target images. While less likely to be affected by local content, the global mechanism can result in mismatches within large regions when the zero-point based correspondence contains errors (see the 1st, 3rd and 4th rows of Fig. 9). Both the methods [15] and [16] solve the image colorization problem by automatically selecting the best color among a set of color candidates via a total variational framework. Method [15] only retains the U and V channels without coupling of the chrominance channels with the luminance, and as a result their regularization algorithm creates halo effects near strong contours, as shown in the 1st, 4th, 7th and 11th rows of Fig. 9. In [16], a strong regularization coupling the luminance and chrominance channels is proposed to preserve the structural information of the image during the colorization process, such as edge and color consistency. It achieves significant

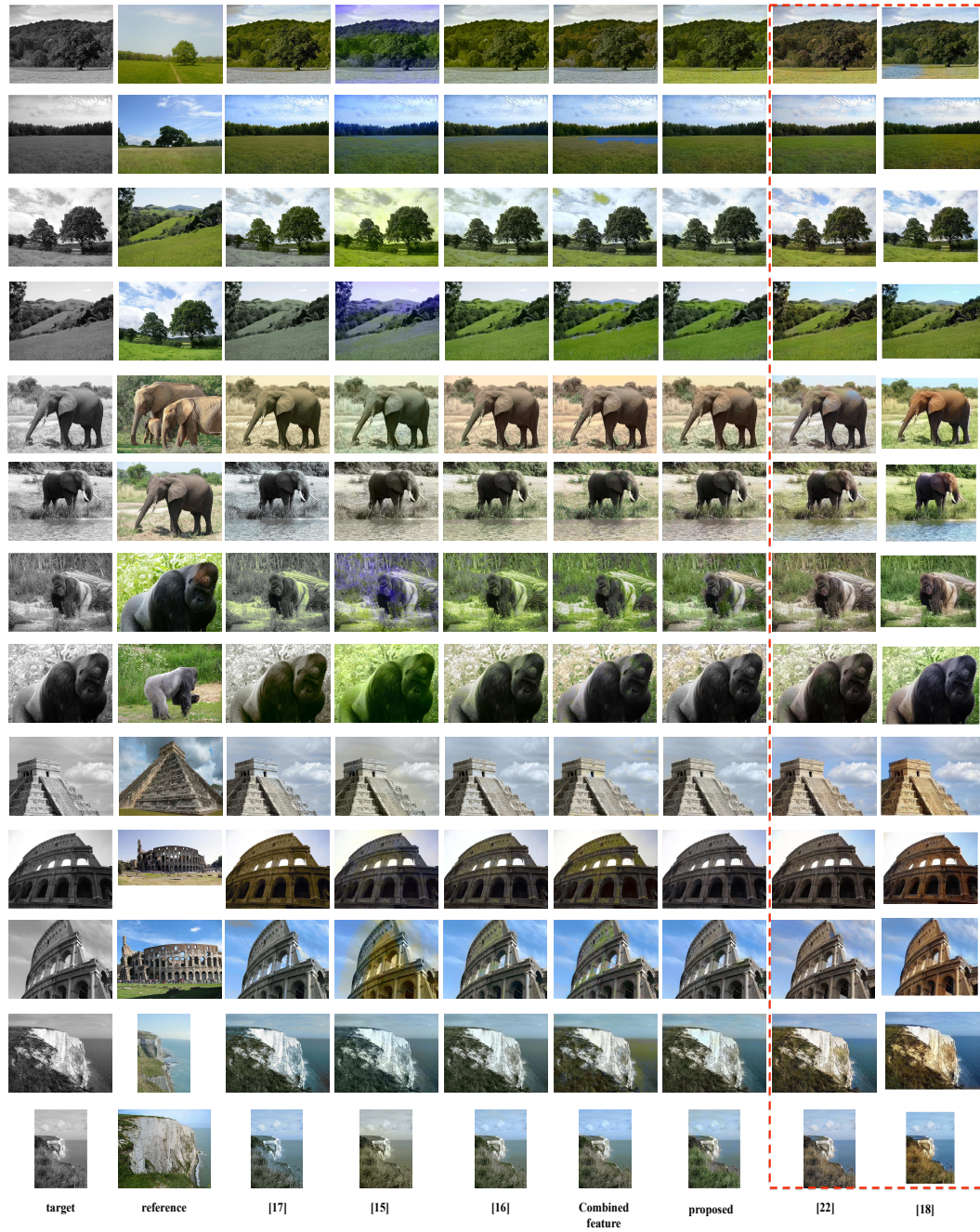


Figure 9: Comparison of our colorization results with alternative methods. From left to right: target and reference images, and the results of different methods.

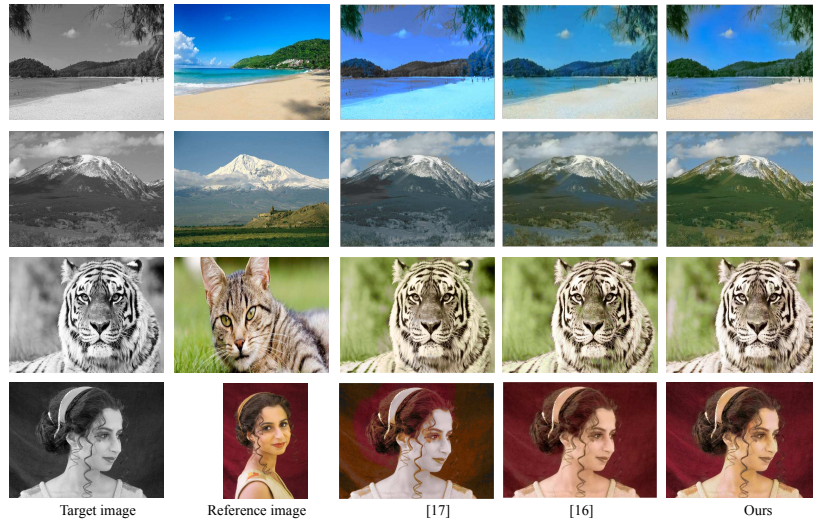


Figure 10: Comparison of our colorization results with alternative example-based colorization methods.

improvement over the method [15]. However, wrong matches remain for challenging scenarios (e.g. 1st-3rd rows of Fig. 9). The sixth column shows the results generated with trivially combined intensity and texture features. We can see that there are numerous incorrect matches, e.g., the green grass is mistakenly matched to the blue sky in the 2nd row of Fig. 9, and the uniform gray sky is mistakenly matched to the grass in the 3rd row of Fig. 9. In contrast, with automatic feature selection using our optimization framework, the proposed method improves color matching substantially and achieves better results as shown in the seventh column.

In addition to example-based methods, we also compare our colorization results against the latest deep-learning based methods [18, 22]. Compared with example-based methods, the deep learning based colorization algorithms use millions of images for training the neural networks. In general, they can generate reasonable color images, as shown in the 8th and 9th columns of Fig. 9. However, there are some obvious artifacts shown e.g. in the 1st and 5th rows where parts of the meadow and elephant are colored in blue. In addition, the output of such deep learning based methods cannot be controlled by the user.

Some colorization results for scenes with complex structure and large color varia-

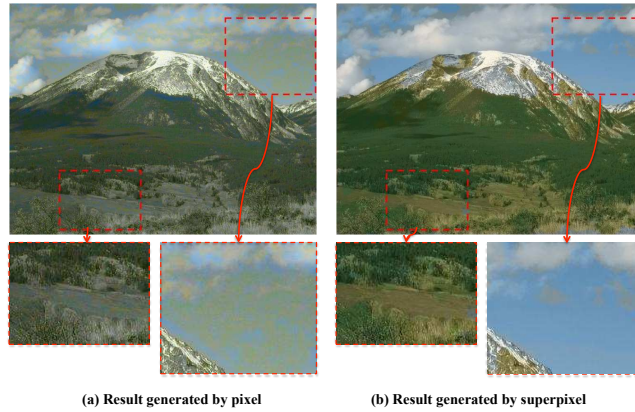


Figure 11: Colorization results by matching of pixels and superpixels.

tions are shown in Fig. 10. These examples are more challenging, as regions with sub-
 355 substantially different colors can have similar local characteristics in grayscale images. We
 compare our results with state-of-the-art example-based colorization methods¹. Due to
 the global mechanism of the method [17], it fails to reproduce correct colors from the
 reference images, as shown in the first two rows of Fig. 10. More specifically, it con-
 fuses the sand beach with the sea (first row) and grass meadow with the sky (second
 360 row), and produces large wrongly colored blue regions. It also generates obvious halo
 effects around the boundary in the third row. The method [16] finds the optimal color
 matching using a variational framework. Thanks to the edge preserving capability of
 the variational function, [16] can reduce the halo effects around the boundary effec-
 tively. However, as only one type of feature is used to find the matching candidates,
 365 many obviously wrong colors are assigned. For example, in the first row, a large por-
 tion of the beach is wrongly colored in blue as it is matched to the sky. This can be
 effectively avoided by using intensity feature in uniform regions as suggested in the
 proposed method. Similar problems can also be found in the remaining examples. In
 comparison, our method produces significantly better results than [15] and [16] for all
 370 of these cases.

¹For this experiment, we compare with methods where code is publicly available, so the result of [15] is not included.

Our method uses superpixels rather than pixels for matching. In this paper, an approximate nearest neighbour (ANN) tree search algorithm is used to find the nearest match. ANN is computationally expensive when the feature dimensionality is high. For example, assuming both the reference image and the target image are of size 300×400 ,
 375 for the 128-dimensional SURF descriptor, it takes *over a day* to find matching pixels by using the fast ANN algorithm². In contrast, if the images are segmented into 4000 superpixels, the ANN algorithm just needs 1.58s. In addition, neighboring pixels in natural images often share similar characteristics, so processing them simultaneously is not only substantially faster, but also improves local coherence and reduces the chance
 380 of mismatches. An example is shown in Fig. 11. To make pixel-based colorization more tractable, we reduce the SURF feature dimension to 30 using PCA (Principal Component Analysis) which generally produces an output with similar quality. However, the ANN step still takes 863.82s, and the result is clearly less coherent than that with superpixels. Based on the above observation, both the reference image and the
 385 target grayscale image are firstly segmented into superpixels.

An additional experiment is designed to evaluate the influence of the number of superpixels. We choose the number of superpixels as 1000, 2000, 4000, 6000 and 8000, and apply our colorization algorithm. Fig. 12 shows the results with different number of superpixels and Table 1 shows the corresponding total running times, where
 390 both target and reference images are of the size 300×400 . It can be seen that when the number of superpixels is too small, e.g., 1000, a superpixel may cover regions of mixed characteristics, which could result in a small number of mismatches. When the superpixel number is larger than 4000, the result is visually similar. However, the computational complexity and running times increase dramatically. In this paper, the
 395 number of superpixels is set to 4000 by default.

Table 1: The running times of our algorithm using different numbers of superpixels.

Number	1000	2000	4000	6000	8000
Time (s)	41.53	73.27	135.07	262.53	381.13

²<http://www.cs.ubc.ca/research/flann/>

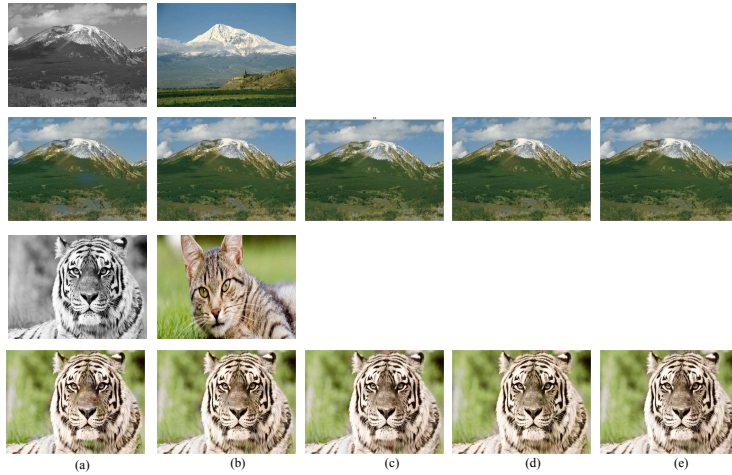


Figure 12: Colorization results with different numbers of superpixels. The first and third rows are the target and reference images. (a)-(e) in the second and fourth rows are the corresponding results with 1000, 2000, 4000, 6000 and 8000 superpixels.

4.2. Quantitative comparisons

In addition to visual inspection, we also make quantitative comparisons for the results shown in Figure 9. In this subsection, the results of deep learning methods [18, 22] are not included. On one hand, deep learning methods use millions of images for training while example-based methods take only one reference image. On the other hand, example-based methods generate results according to the given reference image, whereas the results of deep models are not controlled and thus can be irrelevant to the reference image. We thus focus on comparing our method with state-of-the-art example-based methods in the quantitative analysis to avoid misinterpretation. In this paper, we use the standard Peak Signal to Noise Ratio (PSNR) and Structural SIMilarity (SSIM) [31] as the measurements. Given an $m \times n$ ground truth color image u_0 and the colorization result u , PSNR (in db) is defined as

$$PSNR = 10 \cdot \log_{10} \left(\frac{MAX_I^2}{MSE} \right) \quad (8)$$

Table 2: The quantitative comparisons of different algorithms using the standard PSNR and SSIM measures. I–III are the corresponding results of methods [17, 15, 16], IV are the colorization results obtained by the combined features, and V are the results of the proposed feature selection method. 1–13: corresponding test images as shown in Fig. 9.

	PSNR					SSIM				
	I	II	III	IV	V	I	II	III	IV	V
1	20.91	16.01	21.63	20.71	24.71	0.64	0.25	0.72	0.68	0.79
2	22.66	17.40	22.68	20.91	24.49	0.72	0.39	0.69	0.64	0.75
3	21.03	17.97	24.88	24.03	25.61	0.73	0.39	0.84	0.82	0.87
4	20.28	17.09	26.92	23.58	23.19	0.69	0.45	0.91	0.80	0.87
5	23.38	22.65	24.31	21.36	22.39	0.69	0.65	0.75	0.64	0.68
6	24.39	22.39	24.55	18.18	23.49	0.87	0.75	0.85	0.56	0.83
7	19.78	14.94	21.84	20.84	23.02	0.68	0.37	0.82	0.79	0.83
8	18.37	17.89	18.82	18.37	18.91	0.53	0.51	0.59	0.55	0.63
9	20.17	16.26	18.35	18.07	19.598	0.78	0.30	0.68	0.63	0.76
10	23.93	22.75	31.12	25.15	23.50	0.66	0.42	0.90	0.69	0.79
11	14.33	13.06	14.04	14.31	14.38	0.47	0.33	0.46	0.48	0.49
12	19.76	19.61	20.33	18.40	24.42	0.71	0.64	0.73	0.55	0.85
13	23.06	20.36	25.51	24.59	23.89	0.87	0.54	0.89	0.88	0.86

where MAX_I is the maximum possible pixel value of the image, which is 255 (with standard 8-bit samples). MSE is the mean squared error, which is defined as

$$MSE = \frac{1}{mn} \sum_{i=0}^{m-1} \sum_{j=0}^{n-1} [u(i, j) - u_0(i, j)]^2. \quad (9)$$

SSIM is designed to improve on traditional methods such as PSNR and MSE for better consistency with human visual perception. The scores for different algorithms are shown in Table 2. The quantitative measurements are generally in line with our visual

400 inspection.

4.3. User study

However, since the standard measures are not designed for the task of image colorization, in some cases, visually better results may get worse scores. For example, for the examples in 9th and 10th row of Fig. 9, the results of the proposed method appear more natural by visual inspection, but the PSNR and SSIM scores of our method are lower than those of [16, 17]. Therefore, in order to make a fair comparison, we also perform a user study to quantitatively evaluate our method against other methods.

We designed the user study following the 2AFC (Two-Alternative Forced Choice) paradigm, which is widely used in psychological studies as it is both simple and reliable. 200 users participated in the user study, with ages ranging from 18 to 38. For each test image, every pair of results generated by the different algorithms is shown to the user and he/she is asked to choose the one of them, that looks better. To avoid potential bias, we randomize the order of image pairs shown to the user as well as their left/right position. We record the total number of user preferences (clicks) for each method, and treat these as random variables. The distribution of user preferences for each method is summarized in Fig. 13. Note that since each method is compared with 4 alternative methods, and 13 examples were tested, the maximum number of user preference for each method is 52. The one-way analysis of variance (ANOVA) is used to analyze the user study results. ANOVA is designed to determine whether there exist statistically significant differences between two or more independent groups. ANOVA analysis gives the p-value for the null hypothesis that the means of the groups are equal. Smaller p-value means the groups are more significantly different.

In this paper, the p-values are computed between our method and each alternative method. The results are shown in Table 3. It is clear that all of the p-values are very small which demonstrates the difference between our method and each alternative method is statistically significant, based on the user study. From Fig. 13 we can see that majority of users prefer the method proposed in this paper (Fig. 13 V) which has the highest mean score.

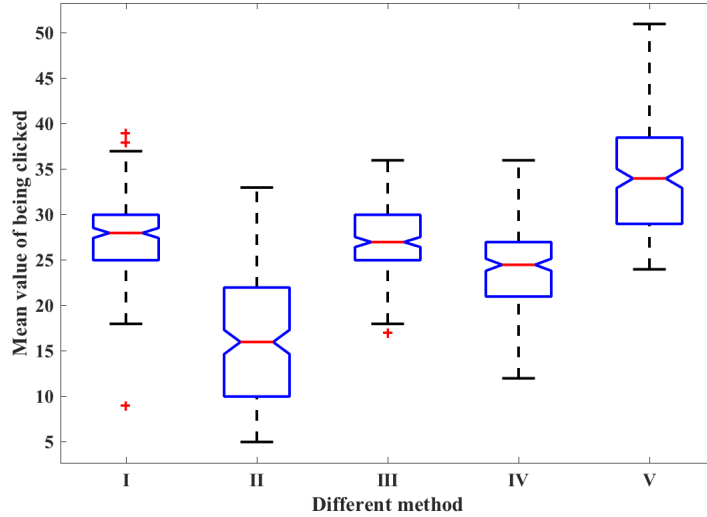


Figure 13: Boxplots of user preferences for different methods, showing the mean (red lines), quartiles (blue lines), and extremes (black lines) of the distributions.

Table 3: The p-values of the ANOVA tests of the proposed method against other methods based on the user study results.

method	I [17]	II[15]	III[16]	IV (combined)
p-value	3.22e-30	2.05e-93	4.09e-38	1.43e-59

5. Conclusion

430 In this paper, we propose a novel approach to image colorization based on auto-
 matic feature selection. By using suitable features for local regions based on their
 uniform/non-uniform characteristics, feature matching quality can be significantly im-
 proved, producing visually better colorization results. To achieve this, Bayesian infer-
 ence is used to estimate the label (type) of each region, and the optimization of feature
 435 selection is effectively formulated using a two-label MRF model. We further use mul-
 tiscale voting and luminance guided image filtering to improve the consistency of the
 final colorization results. By feature selection, our method is able to produce coloriza-
 tion results better than individual features. However, both intensity and texture features
 used are low-level features and may fail to find semantically correct matches. Our

440 method can produce unsatisfactory results in case both features give wrong matches.
To address this, as the idea of using feature selection for improved image coloriza-
tion is general, in addition to the algorithm pipeline proposed in the paper, we would
like to investigate automatic feature selection in alternative colorization frameworks
e.g. by using more robust and semantically meaningful features, as well as for other
445 applications such as color transfer.

Acknowledgements

We would like to thank the authors of [17, 18, 22] for providing their code, and the
authors of [15, 16] for helping to generate comparative experimental results. This work
is funded by natural science foundation of China (NSFC) 61262050, 61562062.

- 450 [1] S. A. Tsafaris, F. Casadio, J.-L. Andral, A. K. Katsaggelos, A novel visualization tool
for art history and conservation: Automated colorization of black and white archival pho-
tographs of works of art, *Studies in Conservation* 59 (3) (2014) 125–135.
- [2] H. Chang, O. Fried, Y. Liu, S. DiVerdi, A. Finkelstein, Palette-based photo recoloring,
ACM Transactions on Graphics (TOG) 34 (4) (2015) 139.
- 455 [3] Y. Chang, S. Saito, K. Uchikawa, M. Nakajima, Example-based color stylization of images,
ACM Transactions on Applied Perception 2 (3) (2006) 322–345.
- [4] T. Welsh, M. Ashikhmin, K. Mueller, Transferring color to greyscale images, *ACM Trans.*
Graph. 21 (3) (2002) 277–280.
- [5] Y. Ling, O. C. Au, J. Pang, J. Zeng, Y. Yuan, A. Zheng, Image colorization via color
460 propagation and rank minimization, in: *International Conference on Image Processing*,
IEEE, 2015, pp. 4228–4232.
- [6] A. Deshpande, J. Rock, D. Forsyth, Learning large-scale automatic image colorization, in:
Proceedings of the IEEE International Conference on Computer Vision, 2015, pp. 567–575.
- [7] Z. Cheng, Q. Yang, B. Sheng, Deep colorization, in: *Proceedings of the IEEE International*
465 *Conference on Computer Vision*, 2015, pp. 415–423.
- [8] A. Levin, D. Lischinski, Y. Weiss, Colorization using optimization, *ACM Trans. Graph.*
23 (3) (2004) 689–694.

- [9] Y.-C. Huang, Y.-S. Tung, J.-C. Chen, S.-W. Wang, J.-L. Wu, An adaptive edge detection based colorization algorithm and its applications, in: *ACM Multimedia*, ACM, 2005, pp. 351–354.
- [10] N. Anagnostopoulos, C. Iakovidou, A. Amanatiadis, Y. Boutalis, S. Chatzichristofis, Two-staged image colorization based on salient contours, in: *International Conference on Imaging Systems and Techniques (IST)*, 2014, pp. 381–385.
- [11] L. Yatziv, G. Sapiro, Fast image and video colorization using chrominance blending, *IEEE Trans. Image Processing* 15 (5) (2006) 1120–1129.
- [12] J. Ying, L. Ji, Pattern recognition based color transfer, in: *International Conference on Computer Graphics, Imaging and Vision: New Trends*, IEEE, 2005, pp. 55–60.
- [13] F. J. Ferri, J. V. Albert, E. Vidal, Considerations about sample-size sensitivity of a family of edited nearest-neighbor rules, *Systems, Man, and Cybernetics, Part B: Cybernetics*, *IEEE Transactions on* 29 (5) (1999) 667–672.
- [14] T. Chen, Y. Wang, V. Schillings, C. Meinel, Grayscale image matting and colorization, in: *Proceedings of Asian Conference on Computer Vision*, Citeseer, 2004, pp. 1164–1169.
- [15] A. Bugeau, V.-T. Ta, N. Papadakis, Variational exemplar-based image colorization, *Image Processing, IEEE Transactions on* 23 (1) (2014) 298–307.
- [16] F. Pierre, J.-F. Aujol, A. Bugeau, N. Papadakis, V.-T. Ta, Luminance-chrominance model for image colorization, *SIAM Journal on Imaging Sciences* 8 (1) (2015) 536–563.
- [17] S. Liu, X. Zhang, Automatic grayscale image colorization using histogram regression, *Pattern Recognition Letters* 33 (13) (2012) 1673–1681.
- [18] R. Zhang, P. Isola, A. A. Efros, Colorful image colorization, in: *European Conference on Computer Vision*, 2016, pp. 649–666.
- [19] A. Y.-S. Chia, S. Zhuo, R. K. Gupta, Y.-W. Tai, S.-Y. Cho, P. Tan, S. Lin, Semantic colorization with internet images, in: *ACM Transactions on Graphics (TOG)*, Vol. 30, ACM, 2011, p. 156.
- [20] X. Liu, L. Wan, Y. Qu, T.-T. Wong, S. Lin, C.-S. Leung, P.-A. Heng, Intrinsic colorization, in: *ACM Transactions on Graphics (TOG)*, Vol. 27, ACM, 2008, p. 152.

- [21] X. Wang, J. Jia, H. Liao, L. Cai, Image colorization with an affective word, in: *Computational Visual Media*, Springer, 2012, pp. 51–58.
- [22] S. Iizuka, E. Simo-Serra, H. Ishikawa, Let there be color!: joint end-to-end learning of global and local image priors for automatic image colorization with simultaneous classification, *ACM Transactions on Graphics (TOG)* 35 (4) (2016) 110.
- 500 [23] D. M. Mount, S. Arya, ANN: library for approximate nearest neighbour searching.
- [24] K. He, J. Sun, X. Tang, Guided image filtering, *IEEE Transactions on Pattern Analysis and Machine Intelligence* 35 (6) (2013) 1397–1409.
- [25] A. Levinstein, A. Stere, K. N. Kutulakos, D. J. Fleet, S. J. Dickinson, K. Siddiqi, Turbopixels: Fast superpixels using geometric flows, *IEEE Transactions on Pattern Analysis and Machine Intelligence* 31 (12) (2009) 2290–2297.
- 505 [26] H. Bay, A. Ess, T. Tuytelaars, L. Van Gool, Speeded-up robust features (SURF), *Computer Vision and Image Understanding* 110 (3) (2008) 346–359.
- [27] J. Li, J. Z. Wang, G. Wiederhold, Classification of textured and non-textured images using region segmentation, in: *Proceedings of International Conference on Image Processing*, Vol. 3, IEEE, 2000, pp. 754–757.
- 510 [28] L. Costantini, L. Capodiferro, M. Carli, A. Neri, Textured areas detection and segmentation in circular harmonic functions domain, in: *IS&T/SPIE Electronic Imaging*, International Society for Optics and Photonics, 2012, pp. 829504–829504.
- [29] Y. Boykov, O. Veksler, R. Zabih, Fast approximate energy minimization via graph cuts, *IEEE Transactions on Pattern Analysis and Machine Intelligence* 23 (11) (2001) 1222–1239.
- 515 [30] Y. Boykov, V. Kolmogorov, An experimental comparison of min-cut/max-flow algorithms for energy minimization in vision, *IEEE Transactions on Pattern Analysis and Machine Intelligence* 26 (9) (2004) 1124–1137.
- 520 [31] Z. Wang, A. C. Bovik, H. R. Sheikh, E. P. Simoncelli, Image quality assessment: from error visibility to structural similarity, *IEEE Transactions on Image Processing* 13 (4) (2004) 600–612.